Molecular Therapy
Original Article

# Increasing the Specificity of AAV-Based Gene Editing through Self-Targeting and Short-Promoter Strategies

Camilo Breton,[1] Thomas Furmanak,[1] Alexa N. Avitto,[1] Melanie K. Smith,[1] Caitlin Latshaw,[1] Hanying Yan,[1] Jenny A. Greig,[1] and James M. Wilson[1]

[1]Gene Therapy Program, Department of Medicine, Perelman School of Medicine, University of Pennsylvania, Philadelphia, PA 19104, USA

**Our group previously used adeno-associated viral vectors (AAVs) to express an engineered meganuclease specific for a sequence in the *PCSK9* gene (M2PCSK9), a clinical target for treating coronary heart disease. Upon testing this nuclease in non-human primates, we observed specific editing characterized by several insertions and deletions (indels) in the target sequence as well as indels in similar genomic sequences. We hypothesized that high nuclease expression increases off-target editing. Here, we reduced nuclease expression using two strategies. The first was a self-targeting strategy that involved inserting the M2PCSK9 target sequence into the AAV genome that expresses the nuclease and/or fusing the nuclease to a specific peptide to promote its degradation. The second strategy used a shortened version of the parental promoter to reduce nuclease expression. Mice administered with these second-generation AAV vectors showed reduced PCSK9 expression due to the nuclease on-target activity and reduced off-target activity. All vectors induced a stable reduction of PCSK9 in primates treated with self-targeting and short-promoter AAVs. Compared to the meganuclease-expressing parental AAV vector, we observed a significant reduction in off-target activity. In conclusion, we increased the *in vivo* nuclease specificity using a clinically relevant strategy that can be applied to other genome-editing nucleases.**

## INTRODUCTION

Gene editing is a powerful technology that can permanently change the genome of target cells in a region of interest. Researchers have leveraged gene-editing nucleases like CRISPR/Cas (clustered regularly interspaced short palindromic repeats [CRISPR]-associated proteins) and meganucleases[1–3] for several important applications, such as understanding the biology of particular genes,[4] improving crop yields and pathogen resistance, and correcting genetic diseases.[5,6]

The proprotein convertase subtilisin/kexin type 9 (*PCSK9*) gene is clinically interesting because its inhibition decreases plasma levels of low-density lipoprotein (LDL) cholesterol—a risk factor in coronary heart disease.[7] Although statin-based therapies are the gold standard for reducing cholesterol levels,[8] there is a growing interest in reducing LDL by inactivating PCSK9. The latter can be achieved, for instance, by using monoclonal antibodies or small interfering RNA (siRNA).[9] The effects of PCSK9 inactivation are not permanent and thus require recurrent dosing. Multiple research groups are trying to develop genome-editing nucleases into a permanent and single-dose treatment that can inactivate PCSK9 and thus reduce LDL.[10–12] This can be achieved by targeting the corresponding nuclease to the coding region of PCSK9 and inducing double-strand breaks (DSBs). The DNA damage is subsequently repaired by different cellular pathways like non-homologous end joining (NHEJ).[13] However, this cellular process is error-prone and can generate insertions and deletions (indels), which can disrupt the open reading frame and prevent the translation of functional PCSK9.

We previously characterized the use of M2PCSK9—an engineered I-Cre-I meganuclease targeting a conserved DNA sequence—in rhesus and human *PCSK9*.[14] We found that in rhesus macaques, a single intravenous injection of an adeno-associated viral vector (AAV) expressing M2PCSK9 reduced circulating PCSK9 levels in a sustained manner.[14] At the molecular level, we observed a dose-dependent formation of indels at the target site. However, a genome-wide analysis of the off-target activity of M2PCSK9 in treated animals revealed that the nuclease also edited other genomic sequences that were homologous to the intended target sequence.[14,15] It is essential to minimize or eliminate the nuclease off-target activity because off-target editing can disrupt genes that are critical for cell viability or controlling cell growth.[16] In this study, we aimed to develop a clinically relevant strategy to reduce M2PCSK9 off-target activity and increase its safety profile without impacting its efficacy.

Although one can engineer the meganuclease amino acid sequence to enhance its specificity,[14,15] this approach is limited. We hypothesized that only a low level of M2PCSK9 nuclease is required to induce

Received 7 October 2020; accepted 18 December 2020;
https://doi.org/10.1016/j.ymthe.2020.12.028.

**Correspondence:** James M. Wilson, Gene Therapy Program, Department of Medicine, Perelman School of Medicine, University of Pennsylvania, 125 South 31st Street, Suite 1200, Philadelphia, PA 19104, USA.
**E-mail:** wilsonjm@upenn.edu

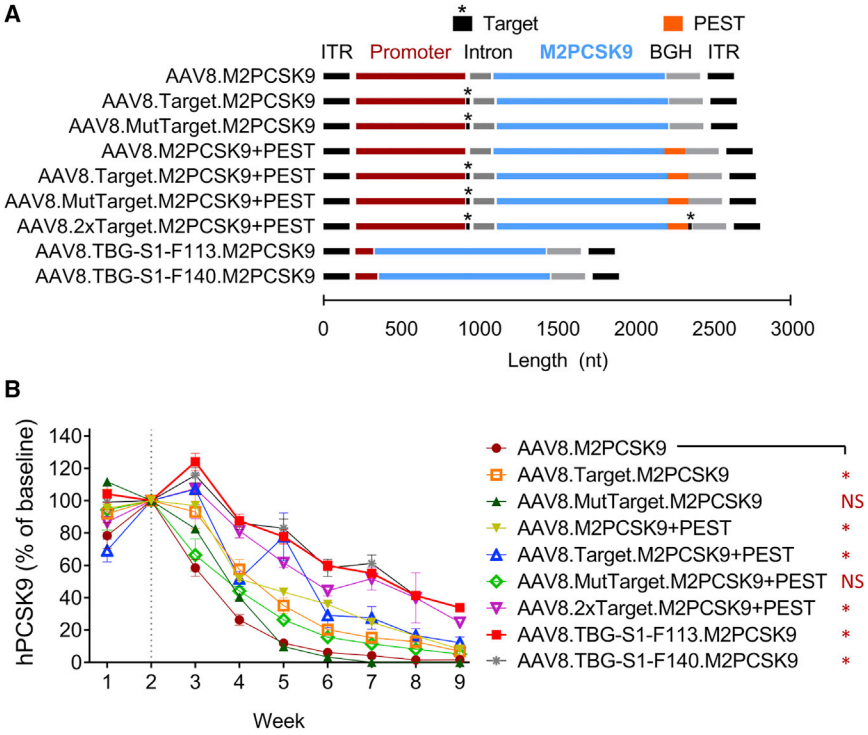


**Figure 1. *In Vivo* Test of Self-Targeting and Short-Promoter AAV**

(A) Schematic representation of the AAV genome of the vectors used in the mouse study. (B) *Rag1* knockout mice were intravenously injected with AAV9.hPCSK9. Two weeks later, mice received an additional dose of the indicated AAV. Circulating hPCSK9 at the indicated time points were quantified and plotted as a percentage of baseline. An asterisk (*) indicates a statistically significant ($p < 0.05$) reduction of hPCSK9 for that group compared to the reduction observed in the AAV.M2PCSK9-treated group; NS, non-significant difference ($p > 0.05$). Data presented as mean ± SEM, n = 5.

editing at the target sequence. Increasing the intracellular nuclease concentration beyond this minimal threshold may increase off-target activity. Thus, our strategy was to reduce cellular nuclease accumulation to reduce off-target activity. We tested two main approaches. The first was a "self-targeting" approach in which the M2PCSK9 target sequence was inserted in the same AAV genome expressing the nuclease to reduce or prevent further transgene expression as a consequence of the self-induced DSBs and/or indels in this target region. An additional "self-targeting" approach consisted of fusing the M2PCSK9 nuclease sequence to a PEST domain (a small peptide rich in proline [P], glutamic acid [E], serine [S], and threonine [T]), which targets the associated protein for degradation.[17–19] The second "short-promoter" approach entailed reducing M2PCSK9 transcription by replacing the highly active, liver-specific human thyroid hormone-binding globulin (TBG) promoter in the parental AAV[14] with shortened versions of TBG. We evaluated the specificity of M2PCSK9 expressed through AAVs containing these regulatory elements in both mice and non-human primates (NHPs). Compared to the parental AAV, we observed reduced M2PCSK9 off-target activity in animals administered with these novel AAV vectors, while the on-target activity was largely conserved.

## RESULTS

### Constructing Self-Targeting and Short-Promoter AAVs with *In Vivo* Editing Capability

In order to obtain the plasmid pAAV.M2PCSK9, we first modified all subsequent plasmids by removing the WPRE sequence in the parental plasmid pAAV.TBG.M2PCSK9.WPRE.BGH[14] (Figure 1A), as this non-coding sequence can lead to a 6- to 8-fold increase in the expression of a transgene.[20,21] To generate "self-targeting" AAV vectors, we inserted the M2PCSK9 target sequence (pAAV.Target.M2PCSK9) immediately after the promoter sequence in pAAV.M2PCSK9. To investigate if the self-targeting activity can be modulated, instead of the M2PCSK9 target sequence, we inserted a mutant target sequence containing eight mismatching nucleotides into the vector genome (pAAV.MutTarget.M2PCSK9). To mediate the expression of a M2PCSK9 nuclease with a reduced half-life, we cloned the PEST sequence in-frame with the carboxyl terminal region of the nuclease (pAAV.M2PCSK9+PEST). Additionally, we generated AAV plasmids that contained a combination of target and PEST sequences (pAAV.Target.M2PCSK9+PEST, pAAV.2xTarget.M2PCSK9+PEST, and pAAV.MutTarget.M2PCKS9+PEST) to investigate whether we can obtain an additive or synergistic effect for improving M2PCSK9 specificity.

We employed a parallel strategy to create shortened versions of the parental TBG promoter to reduce nuclease expression. We constructed two short-promoter AAV plasmids (pAAV.TBG-S1-F113.M2PCSK9 and pAAV.TBG-S1-F140.M2PCSK9) containing only the last 113 and 140 base pairs (bp) of the 3′ end of the TBG promoter. Using these plasmids, we produced AAV vectors and obtained similar AAV titers (Table S1), indicating these modifications did not negatively affect the vector production process.

Given that the M2PCSK9 target sequence is conserved in the rhesus and human genomes but absent from the mouse genome, we tested the *in vivo* editing efficacy of these novel self-targeting and short-promoter AAVs in a pseudo-murine model of human PCSK9. To generate the pseudo-murine model, we injected immune-deficient *Rag1* knockout mice with $3.5 \times 10^{10}$ genome copies (GC)/mouse of AAVs expressing human PCSK9 (AAV9.hPCSK9). We then investigated whether M2PCSK9 activity reduced circulating levels of hPCSK9, which would be indicative of on-target editing in AAV9.hPCSK9. Two weeks after the AAV9.hPCSK9 injection, mice were treated with $10^{11}$ GC/mouse of the different M2PCSK9-expressing AAVs. We collected serum samples at different time

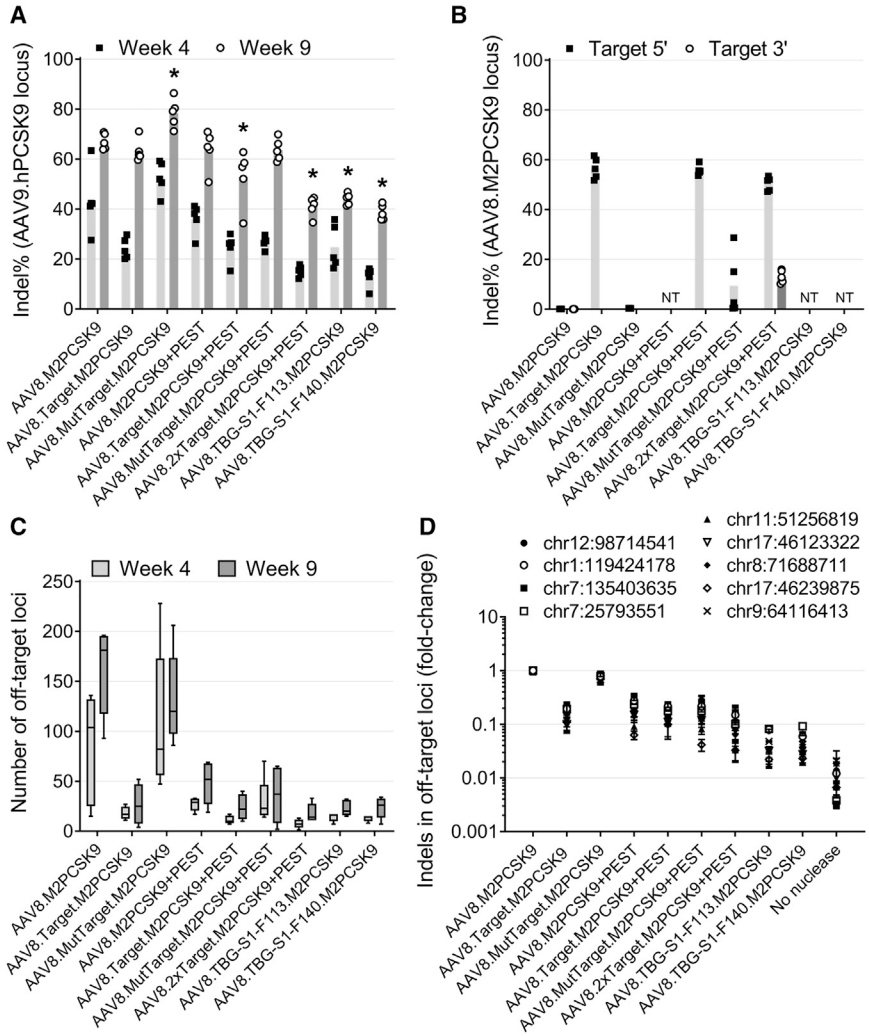


**Figure 2. M2PCSK9 Editing *In Vivo* Expressed by AAV Vectors**

*Rag1* knockout mice treated with AAV9.hPCSK9 and AAV expressing M2PCSK9 were euthanized at either 4 or 9 weeks post-AAV9.hPCSK9. We then isolated liver DNA from the euthanized mice. (A) Indel% in the target region present in AAV9.hPCSK9. (B) Indel% at 9 weeks post-AAV in the target region. (C) Number of M2PCSK9 off-target loci identified by ITR-seq. (D) Indel% in selected top-ranking off-targets at 9 weeks post-AAV. We have indicated the genomic location for each off target. NT, no target sequences were presented in that vector group. Data is shown as mean ± SEM (n = 5). An asterisk (*) indicates groups that are statistically different from the AAV8.M2PCSK9 group ($p < 0.05$, Wilcoxon rank-sum test).

points after vector administration and quantified hPCSK9 levels by a PCSK9-specific enzyme-linked immunosorbent assay (ELISA). Administering the parental AAV8.M2PCSK9 rapidly reduced hPCSK9 in 2 weeks (4r weeks post-AAV9.hPCSK9); moreover, circulating hPCSK9 levels dropped to less than 30% of baseline (Figure 1B). We observed reduced hPCSK9 in the other groups as well, although the kinetics were slower than AAV8.M2PCSK9. The short-promoter AAV (i.e., AAV8.TBG-S1-F113 and AAV8.TBG-S1-F140.M2PCSK9) and the self-targeting AAV8.2xTarget.M2PCSK9+PEST induced the slowest reduction, as they required 7 weeks (9 weeks post-AAV9.hPCSK9) to achieve an hPCSK9 reduction to 30% of baseline (Figure 1B).

### Novel AAV Retains On-Target Activity for M2PCSK9

Next, we investigated whether the different kinetics of hPCSK9 reduction reflected slower editing activity of M2PCSK9 when it was expressed through the novel AAV. DNA was isolated from livers collected at 4 or 9 weeks post-vector-administration. We PCR-amplified a region encompassing the nuclease target site in the AAV9.hPCSK9 vector. Using next-generation sequencing and a custom script, we determined the percentage of amplicons containing indels (indel%; Figure 2). The on-target indel% induced by AAV8.M2PCSK9 was, on average, 43% and 67% at 4 weeks and 9 weeks post-AAV9.hPCSK9 administration, respectively (Figure 2A). We observed a similar indel% at 4 and 9 weeks in the rest of the AAV-treated groups. However, the groups treated with AAV8.2xTarget.M2PCSK9+PEST and the short-promoter AAV presented the lowest editing activity (average indel% of 18% and 41% at 4 and 9 weeks post-AAV, respectively). We also investigated if expressing M2PCSK9 through an even shorter TBG promoter than TBG-S1-F113 (i.e., the last 64 bp of the TBG promoter) still mediated on-target editing. At 9 weeks post-AAV, the average indel% in AAV9.hPCSK9 was 2.5%, which is ~16-fold lower than the average on-target indel% obtained in AAV8.TBG-S1-F113- and TBG-S1-F140.M2PCSK9-treated groups (Figure S1). All together, these data indicate that the modified AAV retained on-target activity with varying editing kinetics.

To investigate if our self-targeting AAVs—which contain the M2PCSK9 target sequence—were recognized and edited by the nuclease, we calculated the indel% in these regions using the PCR-based method described above (Figure 2B). We observed evidence of editing in the target regions present before (5′ target) and after (3′ target) the M2PCSK9 transgene. Whereas indel% was ~60% in the 5′ target in all the target-containing AAVs, editing was only ~13% in the 3′ target, suggesting a nuclease editing preference. The mutant target sequence showed lower levels of more variable editing, in which the indel% was less than 1% in the AAV8.-MutTarget.M2PCSK9 group and between 0.39% to 28.7% for the

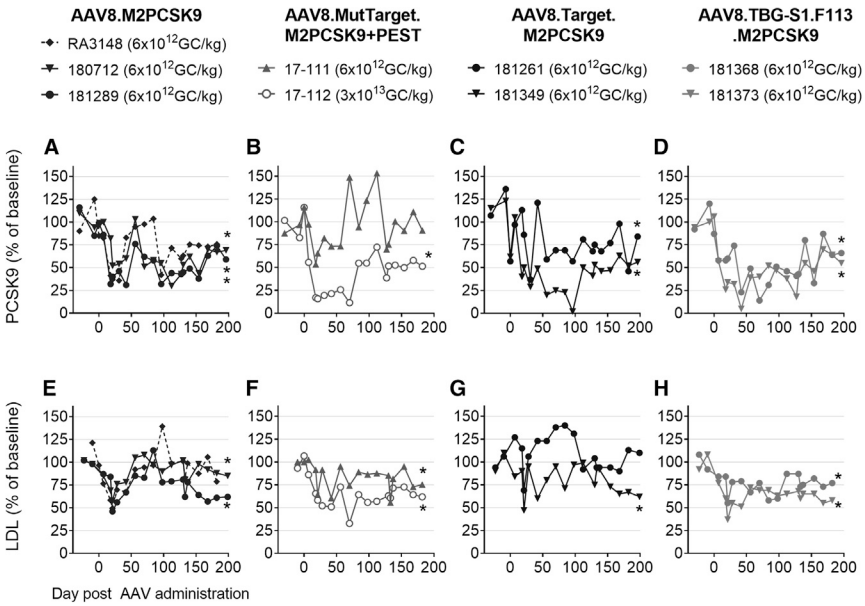


**Figure 3. PCSK9 and LDL Serum Levels at Different Time Points Post-AAV**

(A-F) Here, we show serum PCSK9 (A-D) and LDL (E and F) levels as a percentage of baseline. AAV vector and NHP identification number for each group are displayed on top. An asterisk (*) indicates statistically significant averages (day 56 and until last time point) with respect to average levels pre-AAV dosage ($p < 0.05$, one-sided one-sample t test).

AAV8.MutTarget.M2PCSK9+PEST group at week 9 post-AAV9.hPCSK9 (Figure 2B).

### Evaluating Off-Target Activities of Self-Targeting and Short-Promoter AAVs in Mice

Having characterized the on-target activity, we sought to identify differences in the off-target activity of the expressed M2PCSK9. We performed an unbiased, genome-wide analysis of AAV-treated liver DNA samples using a next-generation sequencing (NGS)-based technique known as ITR-seq.[15] Using this method, we identified an average of 161 different M2PCSK9-edited off-target loci in mice treated with AAV8.M2PCSK9 at 9 weeks post-AAV9.hPCSK9 (Figure 2C). In contrast, there was an ~6-fold reduction in off-targets in the remaining mice treated with AAV at 4 and 9 weeks post-AAV9.hPCSK9 administration (Figure 2C). We observed only a minimal reduction in the number of off-targets in the AAV8.MutTarget.M2PCSK9-treated group (130 off-targets at week 9), suggesting that the mutant target sequence by itself is not enough to reduce the nuclease off-target activity. We performed a more quantitative analysis of these off-targets by analyzing a subset of high-rank off-targets from the ITR-seq results (Table S2; Data S1). We used specific primers to amplify the corresponding off-target genomic locations and calculated the indel% using an NGS analysis of amplicons (Figures 2D and S2). Compared to AAV8.M2PCSK9, the mice treated with AAV8.MutTarget.M2PCSK9 exhibited a 25% reduction in the average off-target indel% (Figure 2D). There was approximately a 9-fold reduction in the off-target indel% in the AAV self-targeting group and an ~20-fold reduction in off-target editing in mice treated with the short-promoter AAV (i.e., AAV8.TBG-S1-F113. and AAV8.TBG-S1-F140.M2PCSK9; see Figure 2D). These data indicate a marked reduction in nuclease off-target activity *in vivo* when nuclease expression is mediated by our novel self-targeting and shortened promoter AAV.

### Retaining M2PCSK9 On-Target Editing Activity in the Novel AAV in NHPs

Encouraged by the data in the pseudo-murine model of human PCSK9, we decided to evaluate the genome-editing activity of some of these AAVs in NHPs. Of importance, at the time of writing, the *in vivo* study was still ongoing for most of the treated NHPs. We selected AAV8.Target.M2PCSK9, AAV8.MutTarget.M2PCSK9+PEST, and AAV8.TBG-S1-F113.M2PCSK9 as they exhibited high on-target and low off-target editing activities; AAV8.M2PCSK9 served as a control. Using previously described methods,[13] we intravenously administered rhesus macaques with a single dose of $6 \times 10^{12}$ GC/kg of each AAV or a higher dose ($3 \times 10^{13}$ GC/kg) of AAV8.MutTarget.M2PCSK9+PEST. A similar extent of liver transduction was observed in all treated NHPs, as we detected comparable numbers of AAV genome copies per diploid cell in liver biopsies obtained at day 18 (d18) (Figure S3A). M2PCSK9 RNA copies were similar among the groups at d18 and d128; by d128, the M2PCSK9 RNA levels decreased for all groups, as shown by two detection methods, qPCR (Figure S3A) and *in situ* hybridization (Figure S3B).

Blood samples were routinely collected from all animals, and liver biopsies were collected on d18 and d128 post-AAV administration. We first evaluated the editing activity of these AAVs by measuring the levels of circulating PCSK9. We compared the average circulating PCSK9 levels for each treated NHP, starting from day 56 up to the latest measurement to the average PCSK9 levels before AAV dosing. There was a significant reduction in PCSK9 to 40%–76% of baseline values in the AAV8.M2PCSK9 and AAV8.Target.M2PCSK9 groups (Figures 3A and 3C, respectively). The higher dose ($3 \times 10^{13}$ GC/kg) of AAV8.MutTarget.M2PCSK9+PEST (Figure 3B) induced a reduction in PCSK9 (47% of baseline), while the $6 \times 10^{12}$ GC/kg dose did not result in a significant PCSK9 reduction. AAV8.TBG-S1-F113.M2PCSK9 reduced PCSK9 to an average level of 49% of baseline after d56 (Figure 3D). We investigated if the nuclease-mediated PCSK9 inhibition reduced LDL cholesterol in treated NHPs. The AAV8.M2PCSK9-treated group showed a small (average of 89% of baseline) reduction in LDL; two NHPs (numbers 180712 and 181289) exhibited a statistically significant reduction in LDL (84% of baseline; Figure 3E). Despite the non-significant PCSK9 reduction in the AAV8.MutTarget.M2PCSK9+PEST group (Figure 3C), the

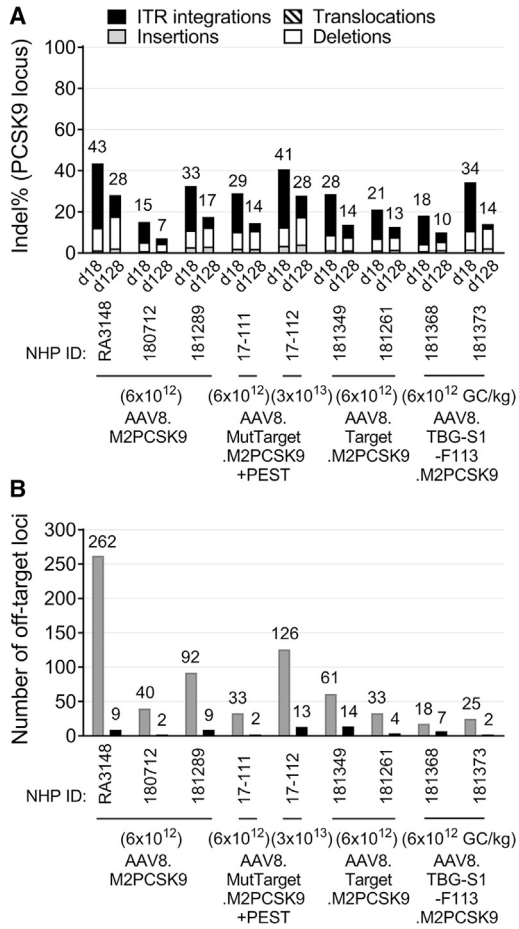


**Figure 4. On- and Off-Target Activity of M2PCSK9 in NHPs**

Rhesus macaques received AAV at the indicated doses. We performed liver biopsies at 18 and 128 days (d18 and d128) post-injection. (A) Indel% in M2PCSK9 target region in the rhesus *PCSK9* gene calculated by AMP-seq. (B) Number of ITR-seq-identified off-targets. Results for d18 (gray bars) and d128 (black bars) liver biopsies are indicated for each NHP.

$6 \times 10^{12}$ GC/kg dose led to a reduction in LDL to 82% of baseline (Figure 3F). Meanwhile, a 5-fold higher dose of this AAV reduced LDL to 61% of baseline. Both reductions were statistically significant ($p < 0.05$, one-sided one-sample t test). In NHPs treated with AAV8.TBG-S1-F113.M2PCSK9, at a dose of $6 \times 10^{12}$ GC/kg, LDL reached 64% and 74% of baseline (Figure 3H), which was the lowest level compared to the other AAV-treated NHPs at the dose of $6 \times 10^{12}$ GC/kg (Figures 3E–3H).

We performed a detailed, molecular-level analysis of the editing in the M2PCSK9 target region using AMP sequencing (AMP-seq), an NGS method capable of detecting small and large indels as well as translocations derived from the editing activity of the nuclease.[14,22] Analysis of liver biopsies at d18 showed a similar editing level between 15% and 43% in all of the NHPs treated with a $6 \times 10^{12}$ GC/kg dose. As expected, a higher dose of AAV8.MutTarget.M2PCSK9+PEST resulted in an increased indel percentage (41%) on d18 (Figure 4A). The most common type of editing in the target region in all of the treated NHPs was integration of sequences derived from the AAV; this type of editing constituted approximately two-thirds of the total indel% at this time point (Figure 4A). In all of the treated NHPs, the percentage of translocation in the on-target region was less than 0.03%. By d128, we observed a reduction of approximately 50% in the on-target editing levels; this was mostly due to a reduction in insertions of sequences matching the AAV vector (ITR integrations; Figure 4A).

### M2PCSK9 Off-Target Activity Is Reduced in Animals Treated with Self-Targeting or Short-Promoter AAVs

We used ITR-seq to test if the reduction in the meganuclease off-target activity observed in mice was also present in NHPs (Figure 4B). As expected, the AAV8.M2PCSK9-treated group showed the highest number of off-targets (average = 131, n = 3) on d18. In NHPs treated with AAV8.MutTarget.M2PCSK9+PEST, AAV8.Target.M2PCSK9, and AAV8.TBG-S1-F113.M2PCSK9, at a dose of $6 \times 10^{12}$ GC/kg, we observed a reduction in the number of off-targets. The greatest reduction in off-targets was in the AAV8.TBG-S1-F113.M2PCSK9 group, where the average number of detected off-targets was 6-fold lower than those in the AAV8.M2PCSK9 group at d18 post-AAV (Figure 4B). However, by d128, most of the off-targets were no longer detectable in liver biopsies from all the treated NHPs; we identified a maximum of 14 off-targets in all the tested NHPs at d128 (Figure 4B). In addition to characterizing the nuclease off-target activity *in vivo*, we also quantified the indel% in a subset of off-targets at d18. From the list of identified off-targets in the treated NHPs, we selected a subset of M2PCSK9 off-targets previously identified by genome-wide, unbiased identification of DSBs enabled by sequencing (GUIDE-seq) *in vitro*.[14,23] We calculated the indel% in amplicons generated from the genomic location of this subset of off-targets (Table 1). The calculated indel in the identified off-target region at d18 was statistically different from untreated cells for some of the selected off-targets (pre versus d18, Table 1). While the indel% in the off-target region was on average 27% at d18 (Figure 4), the indel% in the analyzed off-targets was lower than 1% in almost all the cases (Table 1).

### Immune Responses of Treated NHPs to AAVs

Given that we detected T cells against M2PCSK9-derived peptides in our previous NHP study,[13] we investigated if there was a similar response in these NHPs, as the nuclease expression levels differ between the self-targeting and short-promoter AAVs. We used an interferon (IFN)-γ ELISPOT (enzyme-linked immune absorbent spot) assay to evaluate peripheral blood mononuclear cells (PBMCs) isolated before or on different days post-AAV using pools of peptides derived from the amino acid sequence of the AAV8 capsid or M2PCSK9 (Figure S4). When assayed for peptides derived from the AAV capsid, lymphocytes taken at different time points post-AAV remained mostly negative for T cell activation (Figures S4A, S4C, S4E, and S4G). In contrast, there was a significant activation of T cells in response to M2PCSK9 in lymphocytes collected at different time points post-AAV administration. In two AAV8.M2PCSK9-treated NHPs, this T cell activation remained positive in all the assayed

**Table 1. Indel% in a Subset of M2PCSK9 Off-Targets at Day 18 Post-AAV Injection**

| | AAV8.M2PCSK9 | | | | | | AAV8.MutTarget.M2PCSK9+PEST | | | | AAV8.Target.M2PCSK9 | | | | AAV8.TBG-S1-F113.M2PCSK9 | | | |
|---|---|---|---|---|---|---|---|---|---|---|---|---|---|---|---|---|---|---|
| | $6 \times 10^{12}$ | | | | | | $6 \times 10^{12}$ | | $3 \times 10^{13}$ | | $6 \times 10^{12}$ | | | | $6 \times 10^{12}$ GC/kg | | | |
| | RA3148 | | 180712 | | 181289 | | 17-111 | | 17-112 | | 181349 | | 181261 | | 181368 | | 181373 | |
| | Pre | d18 | Pre | d18 | Pre | d18 | Pre | d18 | Pre | d18 | Pre | d18 | Pre | d18 | Pre | d18 | Pre | d18 |
| 10:72232603 | 0.044 | 0.919[a] | 0.051 | 0.268[a] | 0.053 | 0.057 | 0.025 | 0.462[a] | 0.041 | 0.907[a] | 0.059 | 0.110[a] | 0.070 | 0.326[a] | 0.042 | 0.122[a] | 0.045 | 0.241[a] |
| 5:112049509 | 0.048 | 0.111[a] | 0.049 | 0.064 | 0.055 | 0.050 | 0.041 | 0.062 | 0.052 | 0.098[a] | 0.046 | 0.089[a] | 0.053 | 0.100[a] | 0.045 | 0.048 | 0.051 | 0.065 |
| 19:51609187 | 0.061 | 0.056 | 0.069 | 0.062 | 0.070 | 0.084 | 0.064 | 0.071 | 0.079 | 0.085 | 0.091 | 0.071 | 0.083 | 0.065 | 0.093 | 0.081 | 0.036 | 0.080 |
| 19:31971910 | 0.059 | 0.098[a] | 0.061 | 0.053 | 0.068 | 0.082 | 0.042 | 0.073 | 0.054 | 0.046 | 0.064 | 0.068 | 0.068 | 0.057 | 0.063 | 0.061 | 0.065 | 0.061 |
| 16:48383056 | 0.057 | 0.206[a] | 0.071 | 0.086 | 0.074 | 0.113 | 0.117 | 0.114 | 0.104 | 0.165 | 0.070 | 0.117[a] | 0.085 | 0.078 | 0.082 | 0.053 | 0.068 | 0.070 |
| 16:41164145 | 0.100 | 0.112 | 0.121 | 0.117 | 0.123 | 0.130 | 0.109 | 0.111 | 0.113 | 0.091 | 0.129 | 0.119 | 0.120 | 0.113 | 0.126 | 0.116 | 0.121 | 0.091 |
| 9:53019633 | 0.035 | 0.652[a] | 0.043 | 0.161[a] | 0.041 | 0.288[a] | 0.034 | 0.203[a] | 0.039 | 0.273[a] | 0.034 | 0.069[a] | 0.038 | 0.093[a] | 0.034 | 0.044 | 0.040 | 0.118[a] |
| 14:11716300 | 0.076 | 0.075 | 0.047 | 0.062 | 0.044 | 0.068 | 0.057 | 0.061 | 0.077 | 0.059 | 0.069 | 0.056 | 0.060 | 0.063 | 0.050 | 0.079 | 0.049 | 0.052 |
| 14:69311362 | 0.050 | 0.201[a] | 0.042 | 0.047 | 0.037 | 0.042 | 0.090 | 0.090 | 0.060 | 0.118 | 0.060 | 0.042 | 0.078 | 0.093 | 0.037 | 0.041 | 0.035 | 0.054[a] |
| 7:123575678 | 0.042 | 0.039 | 0.047 | 0.046 | 0.059 | 0.049 | 0.041 | 0.034 | 0.039 | 0.039 | 0.044 | 0.044 | 0.076 | 0.039 | 0.056 | 0.037 | 0.039 | 0.080 |
| 3:169340121 | 0.041 | 0.063 | 0.071 | 0.068 | 0.056 | 0.069 | 0.132 | 0.077 | 0.066 | 0.079 | 0.060 | 0.078 | 0.073 | 0.069 | 0.064 | 0.063 | 0.053 | 0.059 |
| 5:178494083 | 0.058 | 0.075 | 0.073 | 0.075 | 0.052 | 0.059 | 0.066 | 0.059 | 0.049 | 0.050 | 0.066 | 0.056 | 0.066 | 0.081 | 0.066 | 0.059 | 0.091 | 0.084 |
| 16:49265505 | 0.019 | 0.076[a] | 0.032 | 0.046 | 0.031 | 0.026 | 0.043 | 0.043 | 0.042 | 0.028 | 0.067 | 0.058 | 0.059 | 0.084[a] | 0.053 | 0.052 | 0.017 | 0.038[a] |
| 6:2022550 | 0.026 | 0.044[a] | 0.033 | 0.046 | 0.028 | 0.046 | 0.023 | 0.029 | 0.028 | 0.045 | 0.037 | 0.040 | 0.028 | 0.036 | 0.025 | 0.026 | 0.025 | 0.022 |
| 12:30957715 | 0.123 | 0.154 | 0.150 | 0.187[a] | 0.193 | 0.167 | 0.087 | 0.145 | 0.112 | 0.152 | 0.172 | 0.129 | 0.193 | 0.213 | 0.164 | 0.167 | 0.185 | 0.222 |
| 19:5020247 | 0.092 | 0.085 | 0.154 | 0.148 | 0.149 | 0.156 | 0.121 | 0.124 | 0.092 | 0.159 | 0.175 | 0.145 | 0.137 | 0.141 | 0.127 | 0.132 | 0.145 | 0.131 |
| 10:91307547 | 0.098 | 0.115 | 0.133 | 0.169[a] | 0.152 | 0.169 | 0.102 | 0.111 | 0.109 | 0.122 | 0.177 | 0.156 | 0.157 | 0.153 | 0.122 | 0.136 | 0.130 | 0.129 |
| 10:60617626 | 0.017 | 0.014 | 0.053 | 0.038 | 0.045 | 0.043 | 0.029 | 0.024 | 0.022 | 0.036 | 0.034 | 0.039 | 0.039 | 0.029 | 0.026 | 0.021 | 0.030 | 0.024 |
| 10:84231762 | 0.026 | 0.045[a] | 0.034 | 0.032 | 0.034 | 0.027 | 0.034 | 0.023 | 0.025 | 0.035 | 0.027 | 0.028 | 0.024 | 0.028 | 0.019 | 0.027 | 0.020 | 0.029 |
| 10:89468970 | 0.080 | 0.090 | 0.065 | 0.117[a] | 0.065 | 0.079 | 0.080 | 0.058 | 0.071 | 0.085 | 0.060 | 0.067 | 0.066 | 0.129[a] | 0.047 | 0.062 | 0.062 | 0.080 |
| 10:91788445 | 0.019 | 0.032 | 0.021 | 0.024 | 0.022 | 0.020 | 0.023 | 0.023 | 0.013 | 0.039[a] | 0.019 | 0.016 | 0.018 | 0.019 | 0.018 | 0.020 | 0.031 | 0.058 |
| 11:56273284 | 0.104 | 0.102 | 0.348 | 0.218 | 0.266 | 0.268 | 0.170 | 0.097 | 0.106 | 0.113 | 0.330 | 0.267 | 0.296 | 0.299 | 0.278 | 0.243 | 0.138 | 0.307 |
| 12:3457556 | 0.033 | 0.080[a] | 0.041 | 0.057 | 0.052 | 0.074[a] | 0.045 | 0.082[a] | 0.041 | 0.078[a] | 0.045 | 0.045 | 0.047 | 0.043 | 0.055 | 0.064 | 0.043 | 0.052 |
| 1:46715830 | 0.142 | 0.089 | 0.133 | 0.119 | 0.151 | 0.033 | 0.134 | 0.128 | 0.105 | 0.122 | 0.131 | 0.145 | 0.147 | 0.114 | 0.158 | 0.134 | 0.149 | 0.109 |

(*Continued on next page*)

**Table 1. *Continued***

| | AAV8.M2PCSK9 | | | | AAV8.MutTarget.M2PCSK9+PEST | | | | AAV8.Target.M2PCSK9 | | | | AAV8.TBG-S1-F113.M2PCSK9 | | | |
|---|---|---|---|---|---|---|---|---|---|---|---|---|---|---|---|---|
| | $6 \times 10^{12}$ | | | | $6 \times 10^{12}$ | | $3 \times 10^{13}$ | | $6 \times 10^{12}$ | | | | $6 \times 10^{12}$ GC/kg | | | |
| | RA3148 | | 180712 | | 181289 | | 17-111 | | 17-112 | | 181349 | | 181261 | | 181368 | | 181373 | |
| | Pre | d18 | Pre | d18 | Pre | d18 | Pre | d18 | Pre | d18 | Pre | d18 | Pre | d18 | Pre | d18 | Pre | d18 |
| 16:1096991 | 0.114 | 0.237[a] | 0.145 | 0.136 | 0.025 | 0.075 | 0.118 | 0.103 | 0.111 | 0.106 | 0.113 | 0.128 | 0.147 | 0.154 | 0.117 | 0.124 | 0.156 | 0.144 |
| 16:66194026 | 0.073 | 0.280 [a] | 0.094 | 0.202[a] | 0.107 | 0.147 | 0.080 | 0.121 | 0.068 | 0.259[a] | 0.091 | 0.122 | 0.086 | 0.097 | 0.077 | 0.142 | 0.108 | 0.199 |
| 17:95241508 | 0.049 | 0.144[a] | 0.050 | 0.050 | 0.051 | 0.059 | 0.057 | 0.090[a] | 0.056 | 0.137[a] | 0.045 | 0.066 | 0.029 | 0.031 | 0.056 | 0.055 | 0.053 | 0.028 |
| 19:38380297 | 0.072 | 0.269[a] | 0.050 | 0.038 | 0.065 | 0.163 | 0.055 | 0.128[a] | 0.057 | 0.236[a] | 0.061 | 0.082 | 0.073 | 0.153 | 0.047 | 0.082 | 0.065 | 0.265 |
| 19:43980091 | 0.049 | 0.127[a] | 0.104 | 0.058 | 0.090 | 0.080 | 0.057 | 0.045 | 0.047 | 0.129[a] | 0.082 | 0.066 | 0.056 | 0.069 | 0.047 | 0.098 | 0.068 | 0.052 |
| 19:7728843 | 0.056 | 0.285[a] | 0.038 | 0.046 | 0.053 | 0.120[a] | 0.061 | 0.070 | 0.044 | 0.320[a] | 0.037 | 0.073 | 0.041 | 0.032 | 0.029 | 0.064 | 0.021 | 0.072 |
| 20:41111965 | 0.082 | 0.104 | 0.110 | 0.098 | 0.099 | 0.105 | 0.074 | 0.075 | 0.078 | 0.096 | 0.102 | 0.099 | 0.086 | 0.103 | 0.109 | 0.074 | 0.079 | 0.065 |
| 20:66575738 | 0.060 | 0.135[a] | 0.060 | 0.089[a] | 0.065 | 0.165[a] | 0.057 | 0.071 | 0.044 | 0.064[a] | 0.051 | 0.073[a] | 0.053 | 0.076[a] | 0.054 | 0.063 | 0.061 | 0.091 |
| 2:51791846 | 0.041 | 0.106[a] | 0.067 | 0.060 | 0.089 | 0.041 | 0.061 | 0.064 | 0.055 | 0.063 | 0.037 | 0.063 | 0.055 | 0.048 | 0.069 | 0.059 | 0.076 | 0.075 |
| 3:75646081 | 0.008 | 0.044 | 0.041 | 0.037 | 0.044 | 0.040 | 0.021 | 0.041 | 0.023 | 0.000 | 0.044 | 0.040 | 0.036 | 0.043 | 0.038 | 0.031 | 0.042 | 0.032 |

Rhesus macaques were treated with the selected AAV vectors at the indicated dose. For each NHP (NHP ID shown below the dose) and for each off-target location (first column), the indel% in PBMC before AAV treatment (pre) and in liver DNA at 18 days post-AAV treatment (d18) was calculated.
[a]d18 values that are statistically higher than values from control cells (pre) for the corresponding NHP ($p < 0.05$, Fisher's exact test) for each off-target.

time points (Figure S4B). Interestingly, in the NHPs treated with AAV8.MutTarget.M2PCSK9+PEST at a dose of $6 \times 10^{12}$ GC/kg, there was T cell activation in response to the meganuclease peptide pool in PBMCs collected at day 56, but not at later time points (Figure S4D). We observed a similar momentary response in one NHP treated with AAV8.TBG-S1-F113.M2PCSK9 (Figure S4H).

We also quantified the levels of liver transaminases after AAV administration. One of the NHPs treated with AAV8.M2PCSK9 presented a maximum elevation of alanine aminotransferase (ALT) of 1,112 U/L, while the other two NHPs exhibited a maximum ALT elevation of 216 and 162 U/L. On the other hand, AAV8.TBG-S1-F113.M2PCSK9 induced a more modest ALT elevation, with a maximum of 39 and 125 U/L on days 98 and 57 post-AAV, respectively (Figure 5). Aspartate aminotransferase (AST) elevation was similar in the treated animals. Only the AAV8.M2PCSK9-treated NHPs—with the highest ALT elevation—exhibited AST levels higher than 300 U/L (Figure 5).

## DISCUSSION

We have successfully increased the specificity of M2PCSK9 by mediating its expression through self-targeting and short-promoter AAV vectors. Using a pseudo-murine model of hPCSK9 and NHPs, we showed that all the tested AAV vectors mediated expression of the M2PCSK9 nuclease with similar on-target activity and relatively low off-target activity. Given that our approach is based on the regulatory elements presented in the AAV genome and not in modifying the nuclease-coding sequence, we believe that these strategies could be applied to meganucleases targeting other genes. Other groups have used similar strategies to increase the specificity of different nucleases. For instance, multiple research groups achieved transient Cas9 expression in self-targeting lentivirus[24] and AAVs[25,26] by including additional guide RNA in the vectors to target and disrupt the Cas9 transgene. Similar to our strategy, this self-targeting AAV-Cas9 system preserved on-target activity while reducing the off-target activity. Although the self-targeting editing decreased Cas9 expression, the number of AAV GC did not decrease. Similarly, we did not observe a decrease in the number of AAV GC for AAV8.Target.M2PCSK9, compared to AAV8.M2PCSK9 in our NHP studies (Figure S3). Therefore, the reduction in M2PCSK9 off-target activity in the self-targeting AAV is most likely through a mechanism other than a reduction in M2PCSK9 DNA/RNA levels. M2PCSK9 recognized and edited the target sequence in the AAV, given that we detected indels in this region (Figure 2A). However, our PCR-based method only detects small indels, which suggests that we may be missing large insertions/deletions in the vector or in the transcribed RNA that could result in a decrease in translation. To elucidate the mechanisms that reduce off-target activity of the nuclease, additional experiments involving full-sequencing of M2PCSK9 transcripts and episomal AAV genomes could help detect large indels.

One important part of our self-targeting approach was the insertion of a PEST sequence. This peptide has been fused to reporter

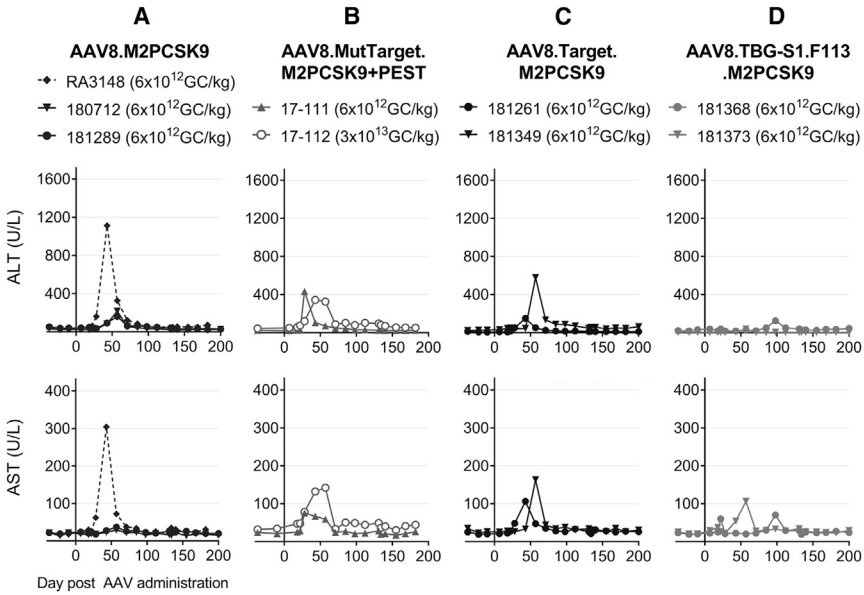


**Figure 5. Liver Transaminase Levels in Treated NHPs**

We quantified ALT (A-D, top row) and AST (A_D, bottom row) in serum samples collected at different times post-AAV. Values are shown as units per liter (U/L). AAV and NHP identification number for each group are displayed on top.

genes to increase their turnover[18] and, as such, was the ideal candidate to directly mediate the reduction in intracellular levels of M2PCSK9. The M2PCSK9+PEST fusion protein reduced off-target activity in mice and NHPs. There was a low, intermittent T cell response to the PEST sequence in NHPs treated with AAV8.Mut Target.M2PCSK9+PEST at a dose of $6 \times 10^{12}$ and $3 \times 10^{13}$ GC/kg (pool C, Figure S4D). While the coding sequence is less than 150 bp, length might be an important factor to consider if a similar approach is used for AAVs that encode larger nucleases like SaCas9.

In the short-promoter approach, the TBG promoter length was reduced from ~700 bp to only 113 bp (Figure 1A). This reduction in the recombinant genome size is of special interest when AAV is used as an expression vector. While the TBG was shortened to arbitrarily chosen lengths, the minimal promoter size for a functional TBG promoter seems to be close to this length, since an AAV expressing M2PCSK9 through a shortened TBG promoter (64 bp) presented an on-target editing of only 2.5% at 9 weeks post-AAV (Figure S1). Nevertheless, compared to the full-length TBG, the transcriptional activity does not seem to be lower for the shortened TBG promoters TBG-S1-F113 and -F140. Indeed, all of the AAV-treated NHPs in our study presented similar M2PCSK9 RNA levels at d18 (Figure S3). Interestingly, while the M2PCSK9 RNA levels were similar for all groups, the number of identified off-targets was higher for the AAV8.M2PCSK9 group than the short-promoter group (AAV8.TBG-S1-F113.M2PCSK9; Figure 4B). As with the AAV8.Target.M2PCSK9 vector, the mechanism for the increased specificity of M2PCSK9 expressed through a short promoter could be related to the sequence of the resulting M2PCSK9 RNA. Elucidating the mechanism for this increased specificity would require characterizing the mRNA produced with full-length and shortened TBG promoters, as well as quantifying M2PCSK9 protein at different times post-AAV treatment; the short-promoter tissue specificity will be determined when the *in vivo* study concludes. Moreover, liver-specific disruption of the *PCSK9* gene can be accomplished using AAV serotypes that target the liver, such as AAV8.[27]

This report represents a step forward in safely translating AAV/meganuclease therapy into the clinic. We identified AAV8.TBG-S1-F113.M2PCSK9 as the most promising candidate for clinical studies as it showed on-target activity that reduced PCSK9 expression and lowered LDL cholesterol while minimizing the nuclease off-target activity, all in stark contrast to the parental AAV8.M2PCSK9 vector. The low elevation in liver transaminases in treated NHPs is an additional important benefit, as minimizing any resulting toxicity represents another important goal in clinical studies. In conclusion, we have developed a set of strategies to increase the specificity of a meganuclease's action in relevant animal models. Future experiments can help determine if this strategy is applicable to other genome-editing nuclease-based therapies.

## MATERIALS AND METHODS

### AAV Plasmids and Vectors

Recombinant AAV vectors were produced by Penn Vector Core at the University of Pennsylvania as previously described.[28] In brief, polyethylenimine was used to transfect AAV *cis*, AAV *trans*, and adenovirus helper plasmids into human embryonic kidney 293 cells. Culture supernatants were collected at 3 days post-transfection, and AAV particles were then purified by iodixanol step gradient. The procedure to clone the vectors used in AAV production is shown below (primer sequences are shown in Table S3).

#### *pAAV.M2PCSK9*

This plasmid is similar to pAAV.TBG.PI.PCS 7-8L.197.WPRE.BGH but without the WPRE sequence.[14] It contains the TBG promoter, a synthetic intron, the coding sequence for M2PCSK9 (I-Cre-I engineered meganuclease, also known as PCS 7-8L.197), and the bovine growth hormone polyadenylation sequence.

#### *pAAV.M2PCSK9+PEST*

The PEST sequence from mouse ornithine decarboxylase was amplified by PCR using the primers PEST-F/-R. We cloned this fragment in Bsu36I-BglII-digested pAAV.TBG.PI.PCS 7-8L.197.WPRE.BGH[14] using an In-Fusion HD kit (Takara, Mountain View, CA, USA) and followed the manufacturer's instructions.

#### *pAAV.Target.M2PCSK9, pAAV.Target.M2PCSK9+PEST, pAAV.MutTarget.M2PCSK9, and pAAV.MutTarget.M2PCSK9+PEST*

We amplified the intron region in pAAV.M2PCSK9 with primers containing either the M2PCSK9 target (C-Target-F/-R primers) or the mutant target (C-MutTarget-F/-R primers) sequences. Fragments with the target or mutant target (MutTarget) sequences were purified and cloned in the PstI and NotI sites of the plasmid that did (pAAV.M2PCSK9+PEST) or did not (pAAV.M2PCSK9) contain the PEST sequence.

#### *pAAV.2xTarget.M2PCSK9+PEST*

We amplified the PEST sequence using the primers PEST-Target-F/-R. The reverse primer contains the additional M2PCSK9 target sequence. We cloned this fragment in the HindIII and BglII sites in p0146 plasmid.[29] We obtained a DNA fragment from this new plasmid by HindIII and XhoI digestion and cloned the fragment in pAAV.Target.M2PCSK9+PEST in the corresponding restriction sites.

#### *pAAV.TBG-S1-F113.M2PCSK9 and pAAV.TBG-S1-F140.M2PCSK9*

We generated shorter versions of the TBG promoter by PCR using the primer TBG-S1-R and either the primer TBG-S1-F113-F or TBG-S1-F140-F. We cloned PCR products in pAAV.M2PCSK9 in the AflII and NotI restriction sites.

### Animal Experiments

All animal procedures were performed in accordance with protocols approved by the Institutional Animal Care and Use Committee of the University of Pennsylvania.

We obtained B6.129S7-Rag1$^{tm1Mom}$/J (also known as Rag1 knockout) mice from The Jackson Laboratory (Bar Harbor, ME, USA). We intravenously administered AAV9.hPCSK9[14] to the mice at a dose of $3.5 \times 10^{10}$ GC/mouse. Two weeks later, mice received an intravenous dose of AAV vectors expressing the corresponding M2PCSK9 nuclease at a dose of $10^{10}$ GC/mouse. Two or seven weeks later (4 or 9 weeks after the initial AAV injection, respectively), mice were euthanized for liver collection.

In NHP studies, we intravenously administered AAV vectors at a dose of $6 \times 10^{12}$ or $3 \times 10^{13}$ GC/kg. We obtained PBMCs and serum samples before and at different times after vector administration. A liver biopsy was collected on d18 post-vector-administration. We performed all the blood tests, including hPCSK9 measurements, as previously described.[14]

### Analyzing On- and Off-Target Activity Using NGS

We calculated the percentage of total alleles containing indels in the region of interest (indel%) using amplicon-seq as previously described.[14] In brief, the region of interest was amplified by PCR using the primers indicated in Table S4. We generated NGS-compatible libraries from the PCR product and subsequently sequenced them on a MiSeq instrument (Illumina, San Diego, CA, USA). These sequences were then mapped to the corresponding reference genome (assembly GRCm38.p6 for mouse and Mmul_8.0.1 for rhesus macaque). Using a custom script, we quantified unedited reads and reads containing indels.[14]

In addition to indels, we quantified AAV integration and translocations in the region of interest by AMP-seq.[14,23] DNA was purified and sheared using a ME220 focused ultrasonicator (Covaris, Woburn, MA, USA) and purified with Agencourt AMPure XP beads (Beckman Coulter, Brea, CA, USA). Fragments were end-repaired, A-tailed, and ligated to special adapters. NGS libraries were generated by two rounds of nested PCR using either the negative (Neg_GSP1 and Neg_GSP2) or positive (Pos_GSP1 and Pos_GSP2) primers, indicated in Table S4. Libraries were sequenced on an Illumina MiSeq. Resulting sequences were mapped to the reference genomes in addition to the sequence of the AAV vector used in the study. Edited alleles were characterized and quantified using a custom script as previously reported.[14]

We carried out an unbiased genome-wide detection of M2PCSK9 off-target sites in the livers of treated mice and NHPs using ITR-seq.[15] Liver DNA was purified and sheared using a ME220 focused ultrasonicator. DNA was end-repaired, A-tailed, and ligated to special adapters as described for AMP-seq. Using AAV-ITR and adaptor-specific primers, we amplified ITR-containing DNA fragments and generated NGS-compatible libraries. We sequenced DNA on a MiSeq and mapped the obtained reads to the reference genome plus the sequence of the AAV vector administered to the animal. We identified off-target sites from the mapped reads using a custom script as described.[15]

### Statistical Analyses

AAV9.hPCSK9 editing in mice was analyzed by Wilcoxon rank-sum test comparing each group against AAV8.M2PCSK9. Reduction in hPCSK9 levels in mice were carried out using linear mixed effect modeling within the R program (v4.0.0) using function "lme" in the "nlme" package. Reduction in rhesus PCSK9 and LDL levels in treated NHPs were determined by performing a one-sided one-sample t test. Indels in selected off-targets were calculated in DNA from liver biopsies taken at d18 post-AAV and in DNA from PBMCs before treatment. These two values were compared using Fisher's exact test. For all the analyses, Benjamini-Hochberg procedure was applied to correct for multiple hypothesis testing.[30] Statistical significance was assessed at the 0.05 level. All the analyses were done using R statistical software (vR.4.0.0)

### Data Availability Statement

All datasets presented in this study are included in the article and Supplemental Information.

## SUPPLEMENTAL INFORMATION

Supplemental Information can be found online at https://doi.org/10.1016/j.ymthe.2020.12.028.

## ACKNOWLEDGMENTS

We thank the Biostatistics and Bioinformatics Core, Immunology Core, Pathology Core, Nucleic Acid Technologies Core, Program

for Comparative Medicine, Vector Core, and the Non-human Primate Research Program of the Gene Therapy Program at the University of Pennsylvania for study support. All vectors were produced by the Penn Vector Core. We also thank Lili Wang, Scott N. Ashley, and Joanna K. Chorazeczewski from the Gene Therapy Program at the University of Pennsylvania for providing us with valuable reagents and/or performing important experiments included in the manuscript. This research was supported by grants awarded to J.M.W. from Precision Biosciences and the University of Pennsylvania, Perelman School of Medicine.

## AUTHOR CONTRIBUTIONS

Conceptualization, C.B. and J.M.W.; Methodology, C.B., J.A.G., and J.M.W.; Formal Analysis, C.B. and H.Y.; Investigation, C.B., T.F., A.N.A., M.K.S., C.L., and J.A.G.; Resources, J.M.W.; Writing Original Draft, C.B. and J.M.W.; Writing – Review & Editing, C.B., J.A.G., and J.M.W.; Supervision, C.B., J.A.G., and J.M.W.; Project Administration, M.K.S.; Funding Acquisition, J.M.W.

## DECLARATION OF INTERESTS

J.M.W. is a paid advisor to and holds equity in Scout Bio and Passage Bio; he holds equity in Surmount Bio; he also has sponsored research agreements with Albamunity, Amicus Therapeutics, Biogen, Elaaj Bio, FA212, Janssen, Moderna, Passage Bio, Regeneron, Scout Bio, Surmount Bio, and Ultragenyx, which are licensees of Penn technology. J.M.W., C.B., and J.A.G. are inventors on patents that have been licensed to various biopharmaceutical companies and for which they may receive payments. None of the other authors declare any other conflicts of interest.

## REFERENCES

1. Arnould, S., Delenda, C., Grizot, S., Desseaux, C., Pâques, F., Silva, G.H., and Smith, J. (2011). The I-CreI meganuclease and its engineered derivatives: applications from cell modification to gene therapy. Protein Eng. Des. Sel. *24*, 27–31.
2. Maeder, M.L., and Gersbach, C.A. (2016). Genome-editing Technologies for Gene and Cell Therapy. Mol. Ther. *24*, 430–446.
3. Hsu, P.D., Lander, E.S., and Zhang, F. (2014). Development and applications of CRISPR-Cas9 for genome engineering. Cell *157*, 1262–1278.
4. Li, X.F., Zhou, Y.W., Cai, P.F., Fu, W.C., Wang, J.H., Chen, J.Y., and Yang, Q.N. (2019). CRISPR/Cas9 facilitates genomic editing for large-scale functional studies in pluripotent stem cell cultures. Hum. Genet. *138*, 1217–1225.
5. Tyagi, S., Kumar, R., Das, A., Won, S.Y., and Shukla, P. (2020). CRISPR-Cas9 system: A genome-editing tool with endless possibilities. J. Biotechnol. *319*, 36–53.
6. Doudna, J.A. (2020). The promise and challenge of therapeutic genome editing. Nature *578*, 229–236.
7. Defesche, J.C., Gidding, S.S., Harada-Shiba, M., Hegele, R.A., Santos, R.D., and Wierzbicki, A.S. (2017). Familial hypercholesterolaemia. Nat. Rev. Dis. Primers *3*, 17093.
8. Adhyaru, B.B., and Jacobson, T.A. (2018). Safety and efficacy of statin therapy. Nat. Rev. Cardiol. *15*, 757–769.
9. Rosenson, R.S., Hegele, R.A., Fazio, S., and Cannon, C.P. (2018). The Evolving Future of PCSK9 Inhibitors. J. Am. Coll. Cardiol. *72*, 314–329.
10. Ding, Q., Strong, A., Patel, K.M., Ng, S.L., Gosis, B.S., Regan, S.N., Cowan, C.A., Rader, D.J., and Musunuru, K. (2014). Permanent alteration of PCSK9 with in vivo CRISPR-Cas9 genome editing. Circ. Res. *115*, 488–492.
11. Carreras, A., Pane, L.S., Nitsch, R., Madeyski-Bengtson, K., Porritt, M., Akcakaya, P., Taheri-Ghahfarokhi, A., Ericson, E., Bjursell, M., Perez-Alcazar, M., et al. (2019). In vivo genome and base editing of a human PCSK9 knock-in hypercholesterolemic mouse model. BMC Biol. *17*, 4.
12. Ran, F.A., Cong, L., Yan, W.X., Scott, D.A., Gootenberg, J.S., Kriz, A.J., Zetsche, B., Shalem, O., Wu, X., Makarova, K.S., et al. (2015). In vivo genome editing using Staphylococcus aureus Cas9. Nature *520*, 186–191.
13. Scully, R., Panday, A., Elango, R., and Willis, N.A. (2019). DNA double-strand break repair-pathway choice in somatic mammalian cells. Nat. Rev. Mol. Cell Biol. *20*, 698–714.
14. Wang, L., Smith, J., Breton, C., Clark, P., Zhang, J., Ying, L., Che, Y., Lape, J., Bell, P., Calcedo, R., et al. (2018). Meganuclease targeting of PCSK9 in macaque liver leads to stable reduction in serum cholesterol. Nat. Biotechnol. *36*, 717–725.
15. Breton, C., Clark, P.M., Wang, L., Greig, J.A., and Wilson, J.M. (2020). ITR-Seq, a next-generation sequencing assay, identifies genome-wide DNA editing sites in vivo following adeno-associated viral vector-mediated genome editing. BMC Genomics *21*, 239.
16. Dai, W.J., Zhu, L.Y., Yan, Z.Y., Xu, Y., Wang, Q.L., and Lu, X.J. (2016). CRISPR-Cas9 for in vivo Gene Therapy: Promise and Hurdles. Mol. Ther. Nucleic Acids *5*, e349.
17. Rogers, S., Wells, R., and Rechsteiner, M. (1986). Amino acid sequences common to rapidly degraded proteins: the PEST hypothesis. Science *234*, 364–368.
18. Li, X., Zhao, X., Fang, Y., Jiang, X., Duong, T., Fan, C., Huang, C.C., and Kain, S.R. (1998). Generation of destabilized green fluorescent protein as a transcription reporter. J. Biol. Chem. *273*, 34970–34975.
19. Ghoda, L., van Daalen Wetters, T., Macrae, M., Ascherman, D., and Coffino, P. (1989). Prevention of rapid intracellular degradation of ODC by a carboxyl-terminal truncation. Science *243*, 1493–1495.
20. Donello, J.E., Loeb, J.E., and Hope, T.J. (1998). Woodchuck hepatitis virus contains a tripartite posttranscriptional regulatory element. J. Virol. *72*, 5085–5092.
21. Powell, S.K., Rivera-Soto, R., and Gray, S.J. (2015). Viral expression cassette elements to enhance transgene target specificity and expression in gene therapy. Discov. Med. *19*, 49–57.
22. Zheng, Z., Liebers, M., Zhelyazkova, B., Cao, Y., Panditi, D., Lynch, K.D., Chen, J., Robinson, H.E., Shim, H.S., Chmielecki, J., et al. (2014). Anchored multiplex PCR for targeted next-generation sequencing. Nat. Med. *20*, 1479–1484.
23. Tsai, S.Q., Zheng, Z., Nguyen, N.T., Liebers, M., Topkar, V.V., Thapar, V., Wyvekens, N., Khayter, C., Iafrate, A.J., Le, L.P., et al. (2015). GUIDE-seq enables genome-wide profiling of off-target cleavage by CRISPR-Cas nucleases. Nat. Biotechnol. *33*, 187–197.
24. Merienne, N., Vachey, G., de Longprez, L., Meunier, C., Zimmer, V., Perriard, G., Canales, M., Mathias, A., Herrgott, L., Beltraminelli, T., et al. (2017). The Self-Inactivating KamiCas9 System for the Editing of CNS Disease Genes. Cell Rep. *20*, 2980–2991.
25. Li, F., Hung, S.S.C., Mohd Khalid, M.K.N., Wang, J.H., Chrysostomou, V., Wong, V.H.Y., Singh, V., Wing, K., Tu, L., Bender, J.A., et al. (2019). Utility of Self-Destructing CRISPR/Cas Constructs for Targeted Gene Editing in the Retina. Hum. Gene Ther. *30*, 1349–1360.
26. Li, A., Lee, C.M., Hurley, A.E., Jarrett, K.E., De Giorgi, M., Lu, W., Balderrama, K.S., Doerfler, A.M., Deshmukh, H., Ray, A., et al. (2018). A Self-Deleting AAV-CRISPR System for *In Vivo* Genome Editing. Mol. Ther. Methods Clin. Dev. *12*, 111–122.
27. Gao, G., Lu, Y., Calcedo, R., Grant, R.L., Bell, P., Wang, L., Figueredo, J., Lock, M., and Wilson, J.M. (2006). Biology of AAV serotype vectors in liver-directed gene transfer to nonhuman primates. Mol. Ther. *13*, 77–87.
28. Lock, M., Alvira, M., Vandenberghe, L.H., Samanta, A., Toelen, J., Debyser, Z., and Wilson, J.M. (2010). Rapid, simple, and versatile manufacturing of recombinant adeno-associated viral vectors at scale. Hum. Gene Ther. *21*, 1259–1271.
29. Wang, L., Bell, P., Lin, J., Calcedo, R., Tarantal, A.F., and Wilson, J.M. (2011). AAV8-mediated hepatic gene transfer in infant rhesus monkeys (Macaca mulatta). Mol. Ther. *19*, 2012–2020.
30. Benjamini, Y., and Hochberg, Y. (1995). Controlling the False Discovery Rate: A Practical and Powerful Approach to Multiple Testing. J. R. Statist. Soc. B *57*, 289–300.

YMTHE, Volume *29*

## Supplemental Information

# Increasing the Specificity of AAV-Based Gene Editing through Self-Targeting and Short-Promoter Strategies

**Camilo Breton, Thomas Furmanak, Alexa N. Avitto, Melanie K. Smith, Caitlin Latshaw, Hanying Yan, Jenny A. Greig, and James M. Wilson**

## Supplemental Figures

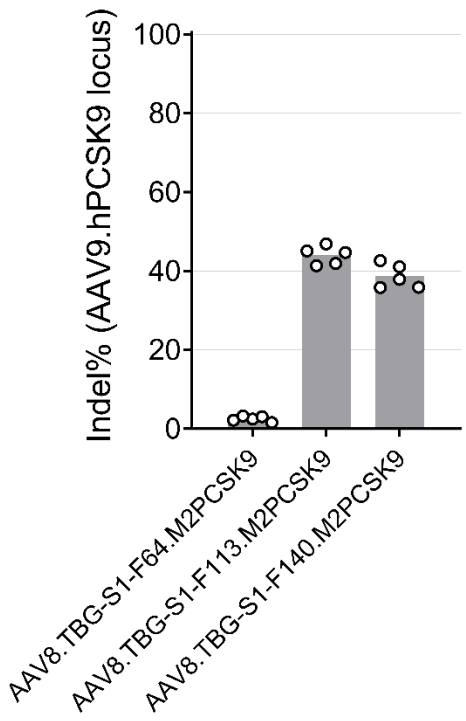


**Figure S1. M2PCSK9 on-target editing in mice treated with shortened-promoter AAV vectors**. *Rag1* knockout mice were treated with AAV9.hPCSK9 and shortened-promoter AAV vectors expressing M2PCSK9. At nine weeks post AAV9.hPCSK9, livers were collected and Indel% in the target region present in AAV9.hPCSK9 was calculated.

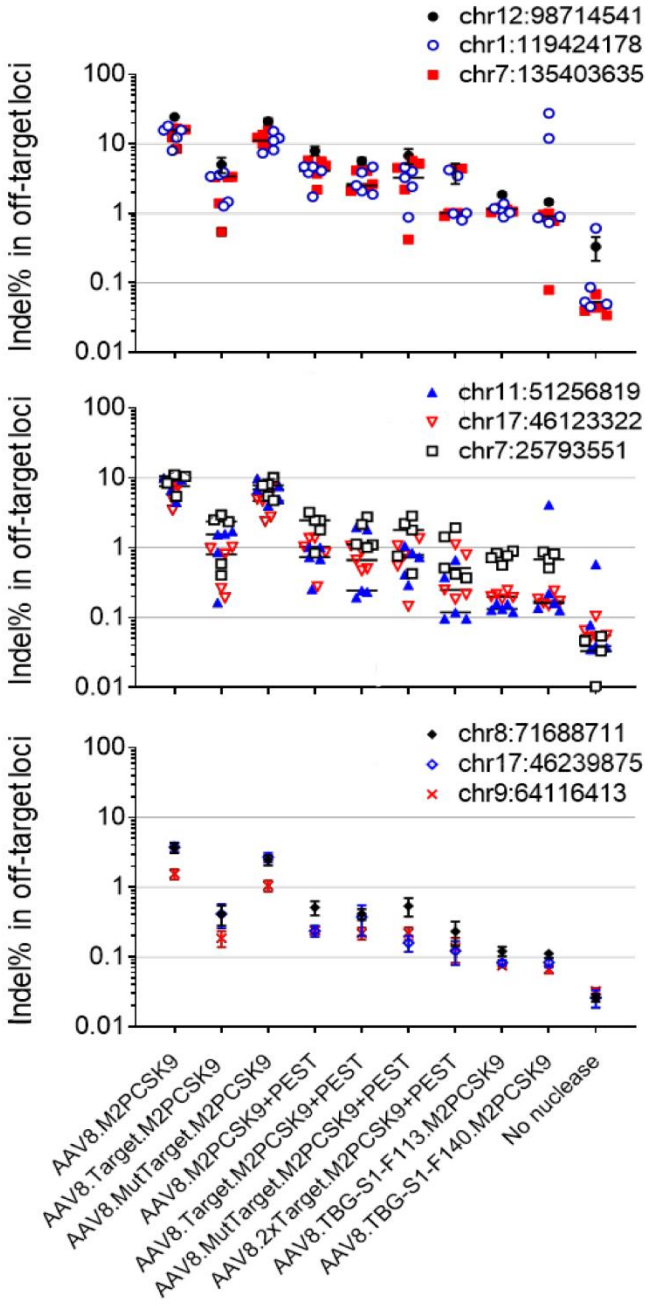


**Figure S2. Editing level in selected off-targets**. ITR-Seq-identified off-targets were ranked according to the number of reads per off-target loci and a subset of nine high-rank off-targets was selected for further NGS analysis. Indel% per mouse is plotted. Off-targets are plotted in groups of three off-targets each to facilitate the visualization.

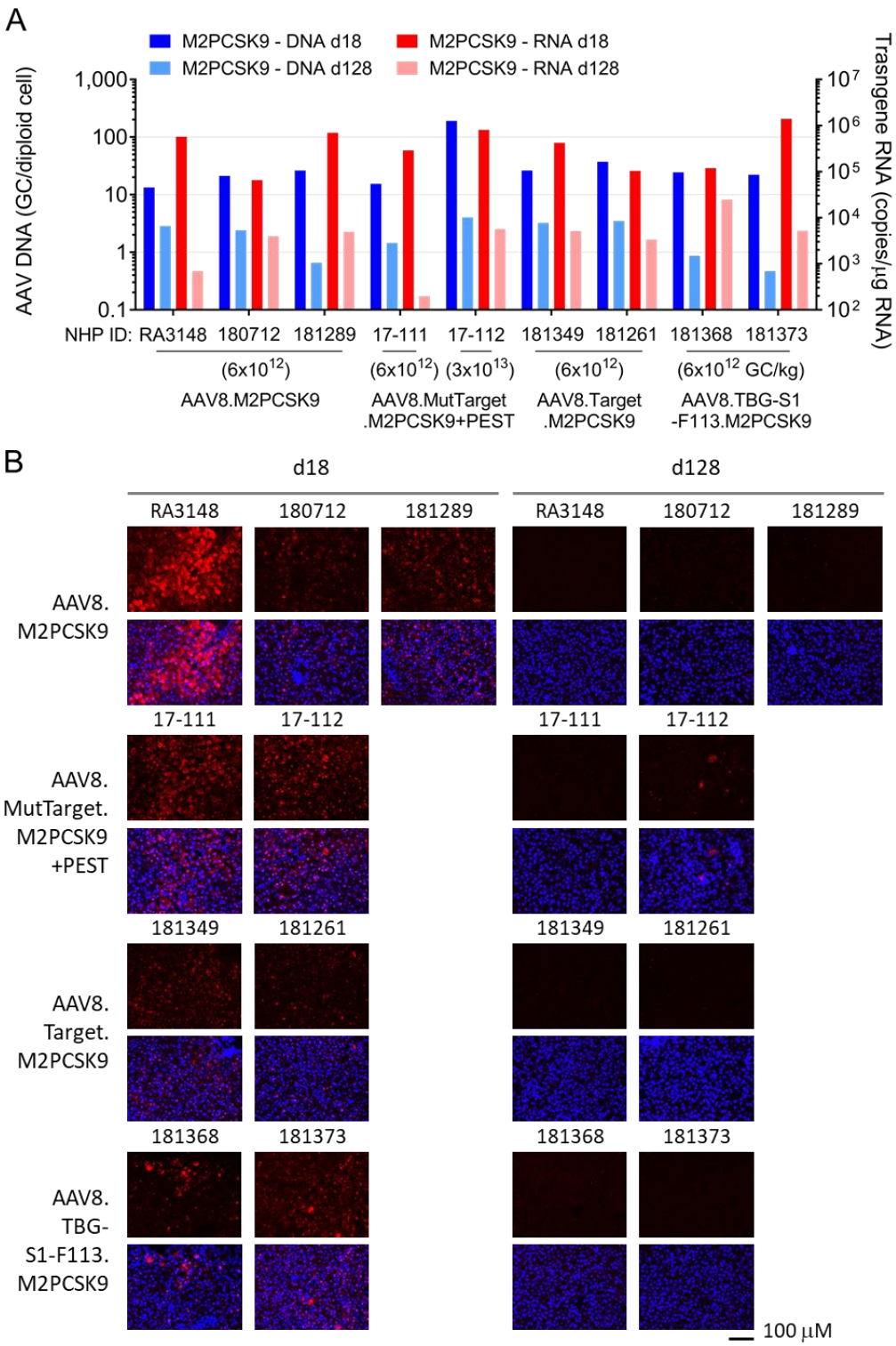


**Figure S3. Liver transduction and transgene RNA expression in NHP. A.** AAV genome copies per diploid cell and M2PCSK9 RNA per microgram of total RNA calculated by qPCR from day 18 or day 128 liver DNA of AAV-treated NHP **B**. In situ hybridization using specific probes to detect M2PCSK9 RNA (red color) along with DAPI nuclei staining (blue) in liver biopsies samples taken at the indicated time points. Scale bar displayed on the bottom right.

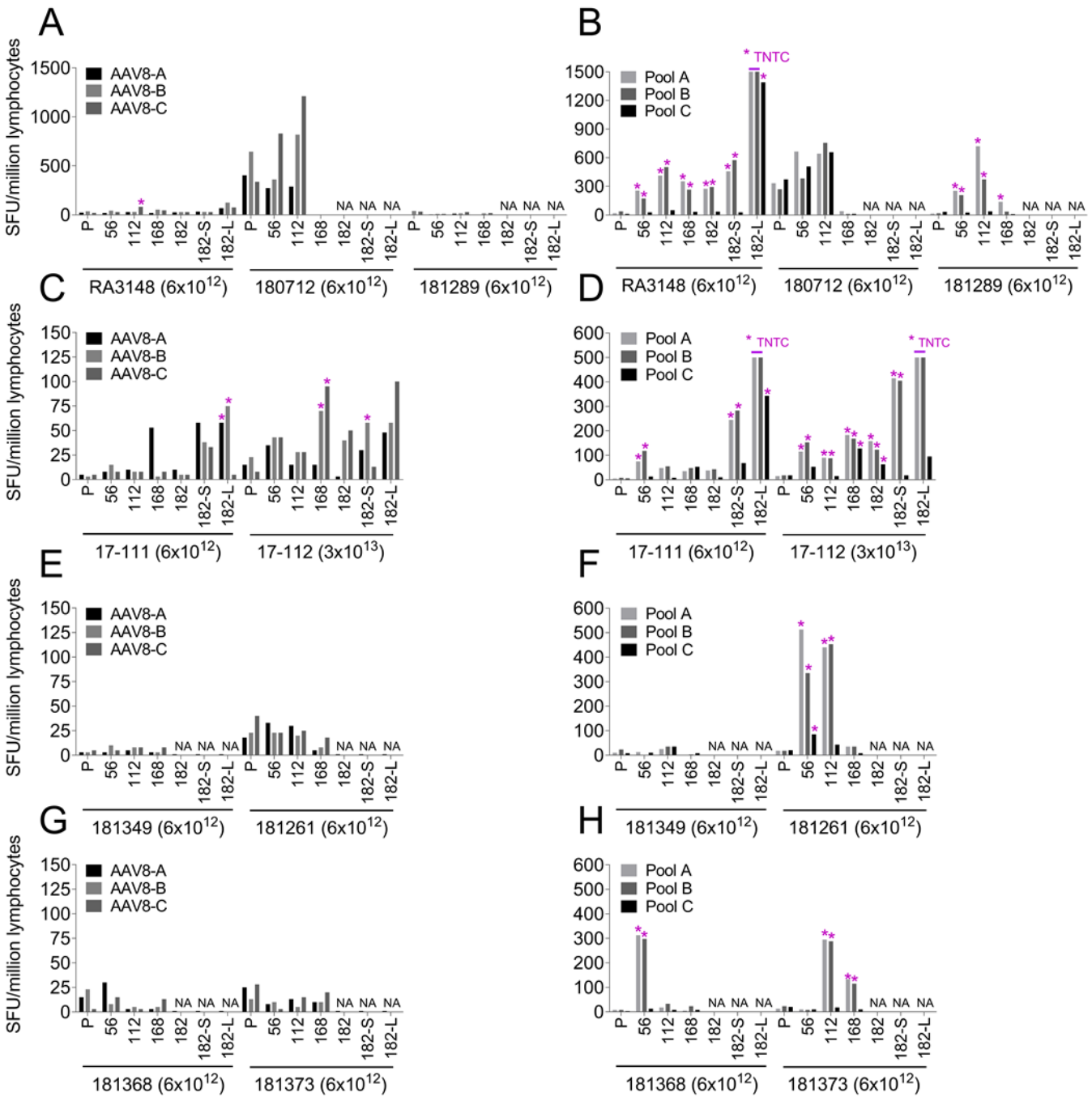


**Figure S4. T-cell responses to AAV8- and M2PCSK9-derived peptide pools.** Number of spot-forming unit (SFU) per million lymphocytes as quantified in the IFN-γ ELISpot using three different pools for AAV8 capsid (AAV8-A, AAV8-B, and AAV8-C) or peptide pools derived from M2PCSK9 sequence (Pool A, Pool B, and Pool C). NHP were treated with AAV8.M2PCSK9 (Panels A and B), AAV8.MutTarget.M2PCSK9+PEST (Panels C and D), AAV8.Target.M2PCSK9 (Panels E and F) or AAV8.TBG-S1-F113.M2PCSK9 (Panels G and H). For the AAV8.MutTarget.M2PCSK9+PEST group, we replaced the Pool C with a peptide pool derived from the PEST amino acid sequence. TNTC, too numerous to count. * indicates a positive T cell activation, defined as >55 SFU per million cells and threefold higher than the negative (medium only) control (P). NA indicates that samples are not available as the study was ongoing. NHP identification number and AAV dose (in GC/kg) are displayed below the timepoints.

## Supplemental Tables

**Table S1. Titers of the produced AAV vectors**

| Vector name | GC/mL | Yield | Cells |
|---|---|---|---|
| AAV8.M2PCSK9 | 9.89E+13 | 2.7E+14 | 3E+9 |
| AAV8.Target.M2PCSK9 | 7.98E+13 | 4.11E+14 | 6E+9 |
| AAV8.MutTarget.M2PCSK9 | 4.89E+13 | 5.74E+13 | 1E+9 |
| AAV8.M2PCSK9+PEST | 5.66E+13 | 6.93E+13 | 1E+9 |
| AAV8.Target.M2PCSK9+PEST | 4.66E+13 | 5.01E+13 | 1E+9 |
| AAV8.MutTarget.M2PCSK9+PEST | 1.07E+14 | 5.53E+14 | 6E+9 |
| AAV8.2XTarget.M2PCSK9+PEST | 8.60E+13 | 1.01E+14 | 1E+9 |
| AAV8.TBG-S1-F113.M2PCSK9 | 1.62E+14 | 8.72E+14 | 6E+9 |
| AAV8.TBG-S1-F140.M2PCSK9 | 1.74E+14 | 9.82E+14 | 6E+9 |

**Table S2. M2PCSK9 off-targets selected for validation.** Bold letters indicate a mismatch to the intended target sequence (5'-TGGACCTCTTTGCCCCAGGGGA-3'), dashes indicate a gap in the off-target sequence and inserted bases are indicated by an underline in the off-target sequence alignment. Ranking was obtained from the ITR-Seq result tables, sorted by number of reads per off-target in descending order.

| | | | Ranking in AAV.M2PCSK9 (week 9) ITR-Seq results | | | | |
|---|---|---|---|---|---|---|---|
| Off-target | Sequence alignment | Target sequence match | Mouse A | Mouse B | Mouse C | Mouse D | Mouse E |
| chr12:98714541 | TG**TC**CCTCT**G**T**C**CCCCAGGG**C**A | 17/22 | 1 | 1 | 1 | 1 | 1 |
| chr1:119424178 | TGG**C**CCTCT**G**TGCCCCAGGG**A**A | 19/22 | 10 | 8 | 7 | 9 | 5 |
| chr7:135403635 | **G**GGACCTCTTT**C**C**T**CCAGGGAGA | 19/22 | 4 | 3 | 3 | 3 | 3 |
| chr7:25793551 | TGGACCTCT**G**T**A**CCCCAG**T**G**T**A | 18/22 | 5 | 4 | 4 | 4 | 5 |
| chr11:51256819 | TGG-CCTCT**C**T--C**A**CAGG**A**GGA | 17/22 | 7 | 5 | 5 | 6 | 7 |
| chr17:46123322 | TG**TC**CCT**T**T**G**T**C**CCCCAGGG**T**A | 16/22 | 11 | 9 | 11 | 11 | 10 |
| chr8:71688711 | TGG**T**CCT**TGGCT**C**G**CCAGGGGA | 15/22 | 3 | 2 | 2 | 2 | 2 |
| chr17:46239875 | TGGACC**CTG**TT**A**CC**AG**AGG**TC**A | 14/22 | 6 | 6 | 6 | 7 | 8 |
| chr9:64116413 | **CAT**ACCTCT**G**T**A**CCCCAGGGGA | 17/22 | 16 | 18 | 8 | 14 | 11 |

**Table S3. Primer sequences used to generate the plasmids for AAV production.** Sequences corresponding to the target or mutant target sequences are in bold.

| **Name** | **Sequence (5' – 3')** |
|---|---|
| C-Target-F | TTGCTTTCTGAGAGACTGCAG**TGGACCTCTTTGCCCCAGGGGA**AAGTTGG TCGTGAGGCAC |
| C-Target-R | TCGCCCTTGCTCACCATGGCGGCCGCTGGACACCTGTGGAGAG |
| C-MutTarget-F | TTGCTTTCTGAGAGACTGCAG**TTGCCCTTTTTATTCCCAGGGA**AAGTTGG TCGTGAGGCAC |
| PEST-F | AGAAGAAGAAGTCGTCCCCCAAGCTTAGCCATGGCTTCCCGCCGGAGGTG GAGGAGCAGGATGATGGCACGCTGCCCATGTCTTGTGCCCAGGAGAGC |
| PEST-R | CTAGAAGGCACAGTCGAGGCTTACTACACATTGATCCTAGCAGAAGCACA GGCTGCAGGGTGACGGTCCATCCCGCTCTCCTGGGCACAAGACATGGG |
| PEST-Target-F | CGGCCTCTTCCGCGTCTTCGAAGCTTAGCCATGGCTTCCCGCCG |
| PEST-Target-R | TAGAAGGCACAGTCGAGGCAGATCTCCCCTGGGGCAAAGAGGTCCATTAC TACACATTGATCCTAGCAGAAGCACAGG |
| TBG-S1-F140-F | TACTTATCTACTTAAGCCTCTTGGCCTTGGTTTTGTACATCAG |
| TBG-S1-F113-F | TACTTATCTACTTAAGCTTTGAAAATACCATCCCAGGGTTAATGCTG |
| TBG-S1-F64-F | TACTTATCTACTTAAGGAGTGCTCTAGTTTTGCAATACAGGACATG |
| TBG-S1-R | CCGCTACACTGCGGCCGCTGTCTCTCAGAAAGC |

**Table S4. Primers used to amplify the region of interest for indel% calculation.**

| Name | Sequence (5' – 3') | Region of interest |
|---|---|---|
| Target_5F | TGCTTTGTTCCTCTTGGCCTTGG | 5' target sequence in AAV vectors |
| Target_5R | TCCTGGCAAAGATGGAACCGTC | |
| Target_3F | GACTCCAAGACCCGCAAGACCACTTC | 3' target sequence in AAV vectors |
| Target_3R | TTATTAGGAAAGGACAGTGGGAGTGGCACC | |
| PCS_MMF | TGCCACCTACCTCCTCACCTTTC | On-target region in rhesus PCSK9 gene |
| PCS_MMR | GGCTGTTAGCATCACGGTGG | |
| AAV_PCS_F | CCTCAGCTCCCGAGGTCATCACAGTTG | On-target region in AAV9.hPCSK9 vector |
| AAV_PCS_R | TGACATCTTTGGCAGAGAAGTGGATCAGTC | |
| Pos_GSP1 | GGATCTCGACGCTCTCCCTCCAGGACCAGCCGGTGAC | AMP-Seq analysis of rhesus PCSK9 gene (positive primers set) |
| Pos_GSP2 | CCTCTCTATGGGCAGTCGGTGATGACCCTGGGGACTTTGGGG | |
| Neg_GSP1 | GGATCTCGACGCTCTCCCTGCAGCAGCCTGCGATGTC | AMP-Seq analysis of rhesus PCSK9 gene (negative primers set) |
| Neg_GSP2 | CCTCTCTATGGGCAGTCGGTGATCGATGTCCCACTCCGTGACAC | |